**ASSOCIATE CONTENT - SUPPORTING INFORMATION**

# Pervasive Genomic Damage in Experimental Intracerebral Hemorrhage: Therapeutic Potential of a Mechanistic Based Carbon Nanoparticle

*Prakash Dharmalingam[1], Girish Talakatta[1], Joy Mitra[1], Haibo Wang[1], Paul J. Derry[2], Lizanne Greer Nilewski[3], Emily A. McHugh[3], Roderic H. Fabian[4], Kimberly Mendoza[3], Velmarini Vasquez[1], Pavana M. Hegde[1], Eugenia Kakadiaris[3], Trenton Roy[3], Istvan Boldogh[6], Venkatesh L. Hegde[1], Sankar Mitra[1,7], James M. Tour[5]*, Thomas A. Kent[2,3,8]* and Muralidhar L. Hegde[1,7,9]**

*[1]Department of Radiation Oncology, Houston Methodist Research Institute, Houston, TX 77030, USA; [2]Institute of Biosciences and Technology, Texas A&M Health Science Center, Houston, TX 77030, USA, [3]Department of Chemistry, Rice University, Houston, Texas 77005; [4]Department of Neurology, Baylor College of Medicine, and Michael E. DeBakey VA Medical Center, Houston, Texas 77030, [5]Departments of Chemistry, Computer Science, Materials Science and NanoEngineering, Smalley-Curl Institute and the NanoCarbon Center, Rice University, Houston, TX 77005, USA; [6]Department of Microbiology and Immunology, University of Texas Medical Branch, Galveston, TX 77555, USA; [7]Weill Medical College of Cornell University, New York, USA; [8]Stanley H. Appel Department of Neurology, Houston Methodist Hospital and Research Institute, Houston, TX 77030, [9]Center for Neuroregeneration, Department of Neurosurgery, Houston Methodist Neurological Institute, Houston Methodist, Houston, TX 77030, USA*

*****Correspondence and requests for materials should be addressed to M.L.H. (email: mlhegde@houstonmethodist.org), J.M.T. (email: tour@rice.edu), or T.A.K. (email: tkent@tamu.edu)

**Supporting Information includes 1 Table, 8 Figures and Supplemental Methods**

**Supporting Table S1.** Gene Targets and Sequences of Primer Pairs used for LA-PCR Experiment.

| Gene | Forward | Reverse |
|---|---|---|
| Human HPRT LA | 5′-TGGGATTACACGTGTGAACCAACC-3′ | 5′-GCTCTACCCTGTCCTCTACCGTCC -3′ |
| Human HPRT SA | 5′-TGCTCGAGATGTGATGAAGG-3’ | 5′-CTGCATTGTTTTGCCAGTGT-3’ |
| Human Mito LA | 5′-TCTAAGCCTCCTTATTCGAGCCGA-3’ | 5′-TTTCATCATGCGGAGATGTTGGATGG-3’ |
| Human Mito SA | 5′-CCCCACAAACCCCATTACTAAACCCA-3’ | 5′-TTTCATCATGCGGAGATGTTGGATGG-3’ |
| Mouse Nuclear LA | 5′-GGACACAGGACGGAGCAATATAAG- 3′ | 5′-CCTGTGAGTGGTCAGGAGTTAAAG- 3′ |
| Mouse Nuclear SA | 5′- GTCCATTAGTCCTGTCCCTTTC - 3′ | 5′- GCAATGGATGCTGGGATACT - 3′ |
| Mouse Mito LA | 5′-GCCAGCCTGACCCATAGCCATAATAT-3′ | 5′-GAGAGATTTTATGGGTGTAATGCGG-3′ |
| Mouse Mito SA | 5′-CCCAGCTACTACCATCATTCAAGT-3′ | 5′-GATGGTTTGGGAGATTGGTTGATGT-3′ |

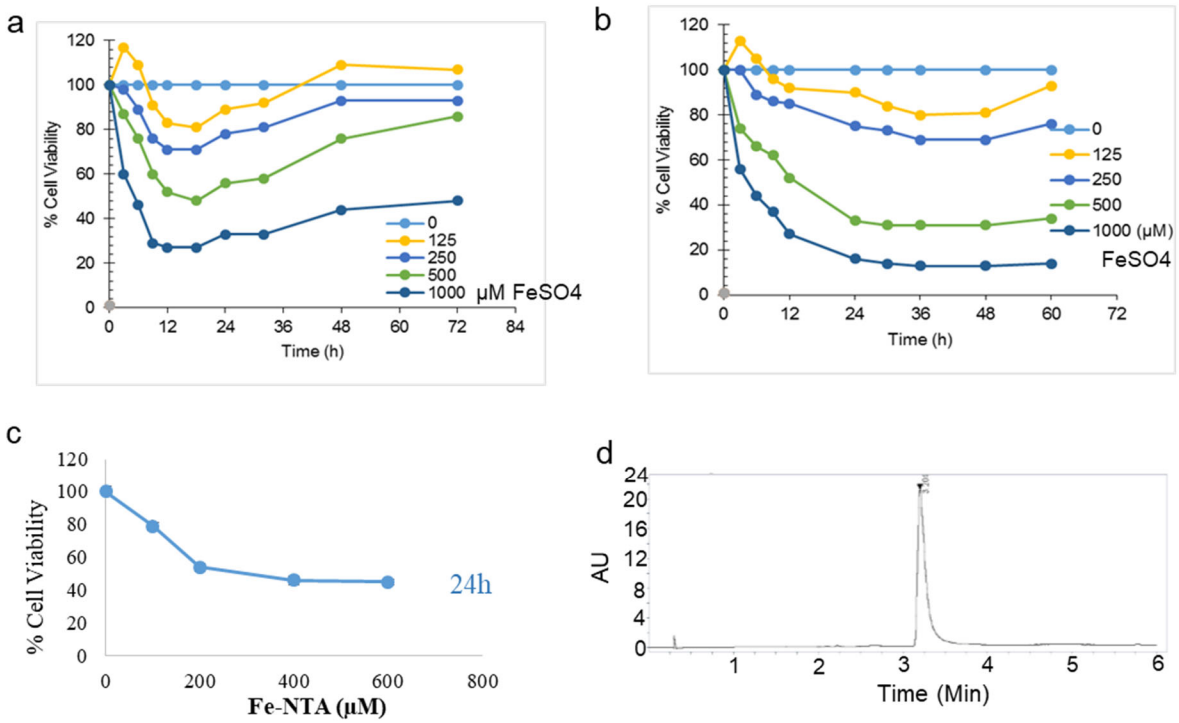


**Figure S1**. Cell viability analysis by MTT assay in undifferentiated SH-SY5Y cells (a) and differentiated neurons (b) in the presence of $FeSO_4$ and determination of $IC_{50}$ value. The cells were treated with increasing doses of iron for 12 h, washed, cultured in fresh media and assayed with MTT at the time indicated. **(c)** Viability of differentiated SH-SY5Y cells with increasing doses of Fe-NTA complex. **(d)** Chromatogram of hemin indicates purity of hemin used in experiments

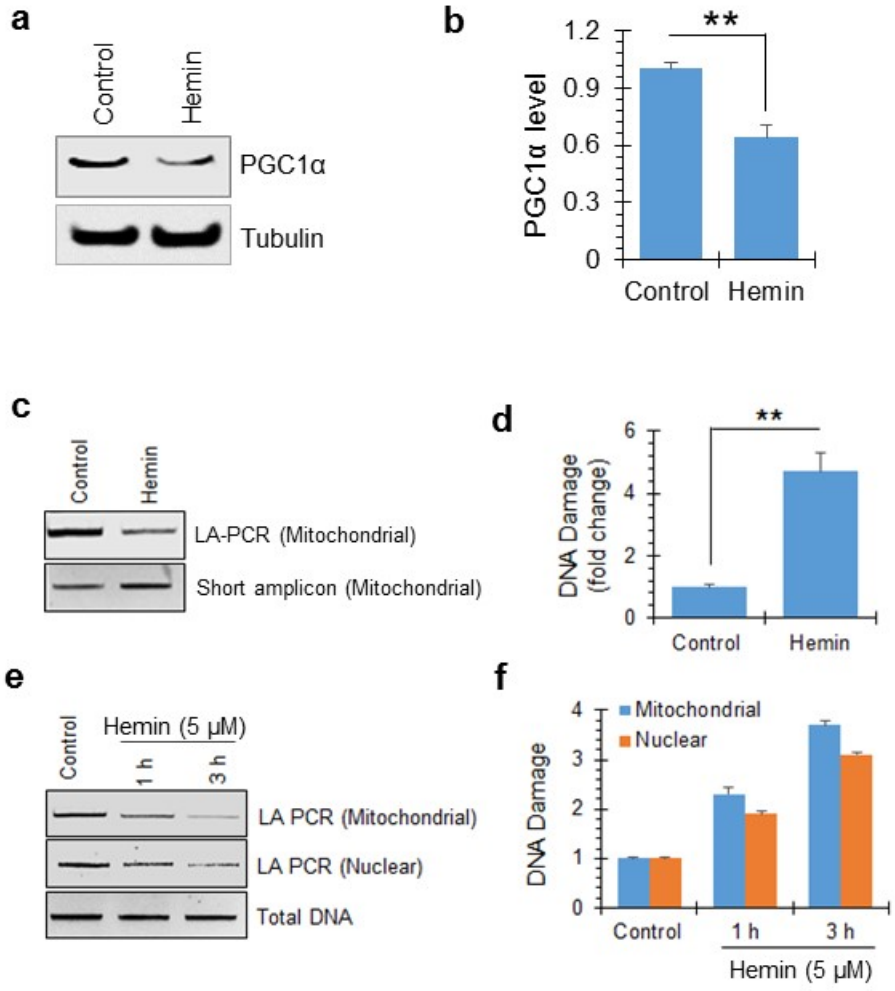


**Figure S2.** (**a** and **b**) IB analysis of PGC-1α expression in differentiated neurons treated with hemin (5 μM) for 12 h. (**c, d**) LA-PCR analysis of mitochondrial DNA extracted from hemin-treated neurons. A 200bp short amplicon PCR served as control. (**e, f**) LA-PCR analysis nuclear and mitochondrial DNA extracted at 1 h and 3 h post hemin treatment. Same amount of total DNA used was shown. Quantitation of DNA damage fold changes, **$p < 0.05$.

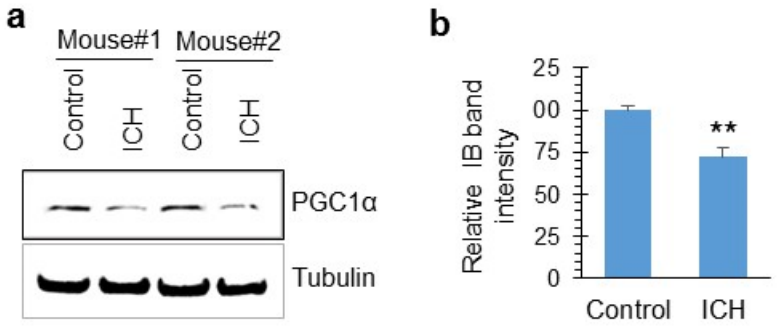


**Figure S3.** (**a** and **b**) IB analysis of PGC1α expression in control and ICH-induced mouse brain extracts. Representative IB from 2 mice shown in (a). Mean IB band intensity quantitation showing reduced PGC1α expression in the ICH (right hemisphere) compared to control (left hemisphere) from 4 mice. **p<0.05.

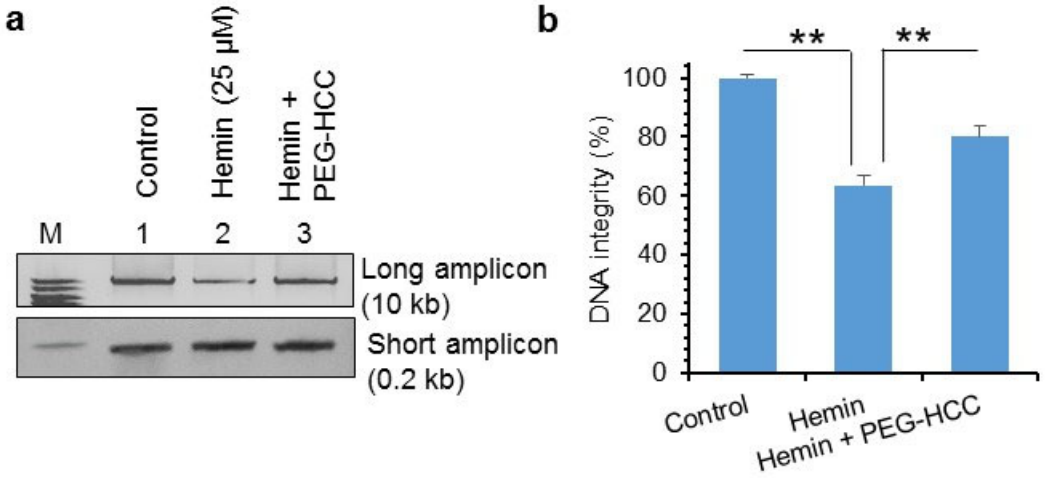


**Figure S4.** (**a** and **b**) LA-PCR analysis of DNA extracted from b.End3 cells treated with hemin and PEG-HCC. Mitochondrial DNA (10 kb) was used as a long amplicon (LA), while 0.2 kb within the LA region was used as a short amplicon (SA). Picogreen-based quantitation of amplified DNA expressed as percent (%) of DNA integrity. **p<0.05.

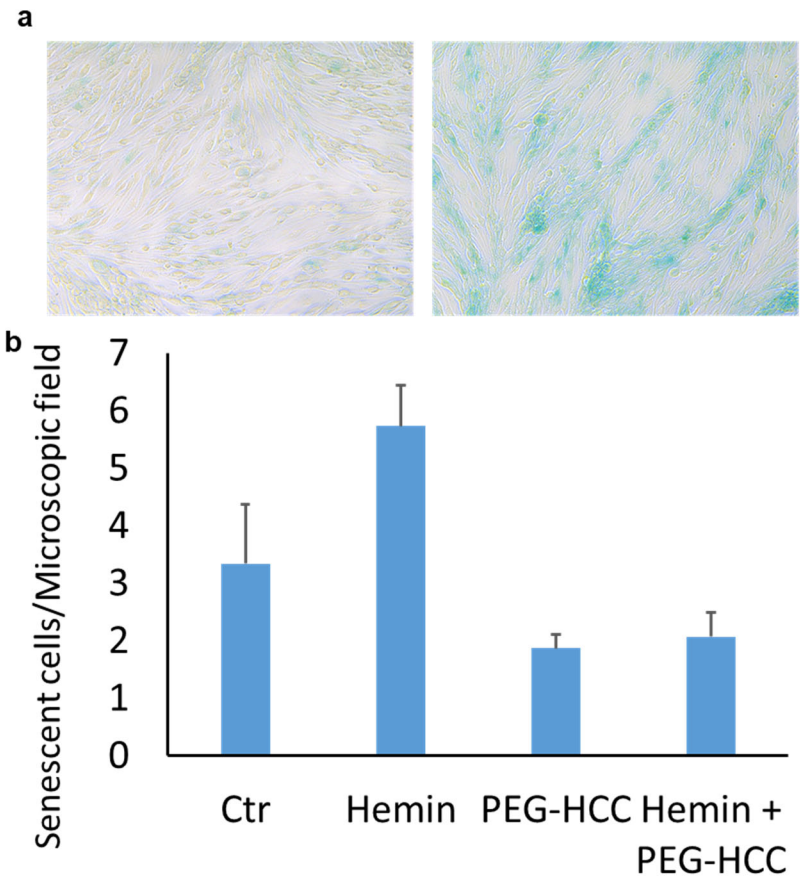


**Figure S5**. Senescence-associated β-galactosidase expression (blue staining) in cultured bEnd.3 brain endothelial cell line after 5 d incubation (equal vibrance settings). **(a)** Left panel: DMSO carrier shows scattered blue cells. Right panel: 50 μM hemin in DMSO with widespread staining. (b) Quantitation of the number of senescent β-gal-positive cells per microscopic field 5 d following treatment. Data are presented as Mean ± SD for 3 independent experiments, 5 microscopic fields per each well were counted.

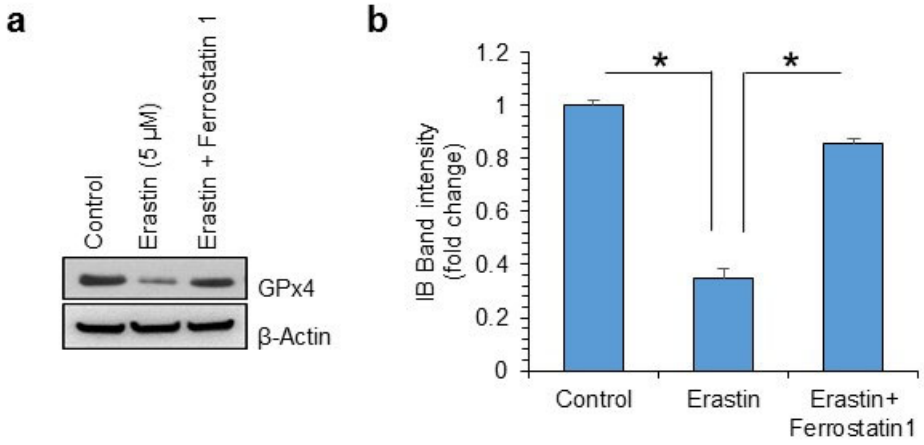


**Figure S6.** (**a**) IB of GPx4 in erastin-treated cells with or without ferrostatin 1 compared to control cells (**b**) Quantitative analysis of GPx4 in iPSC-derived neurons treated with erastin with or without ferrostatin 1 compared to control cells. *$p<0.01$.

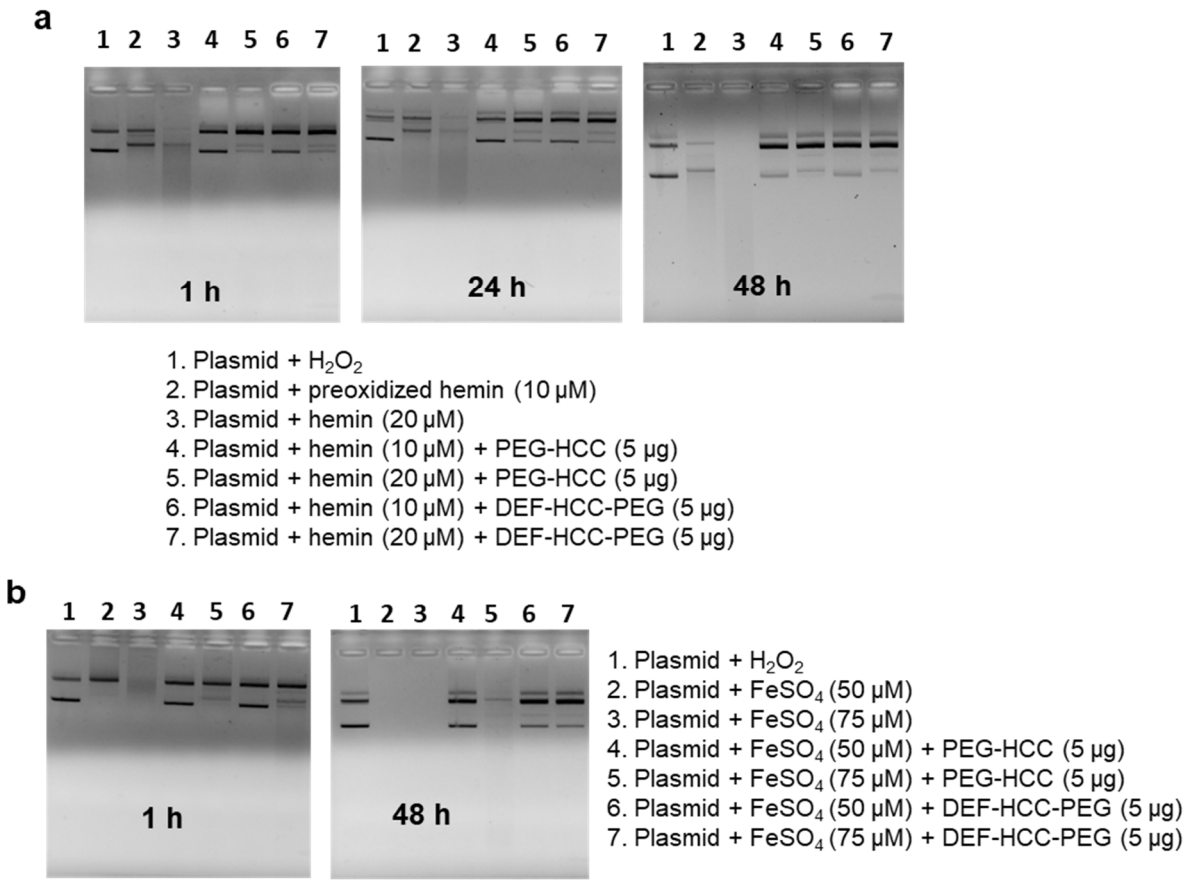


**Figure S7.** (**a**) Agarose gel analysis of plasmid DNA in the presence of pre-oxidized hemin (10 or 20 μM) with or without PEG-HCC and DEF-HCC-PEG *in vitro*. (**b**) Plasmid in the presence of iron (50 or 75 μM) with or without PEG-HCC and DEF-HCC-PEG *in vitro*.

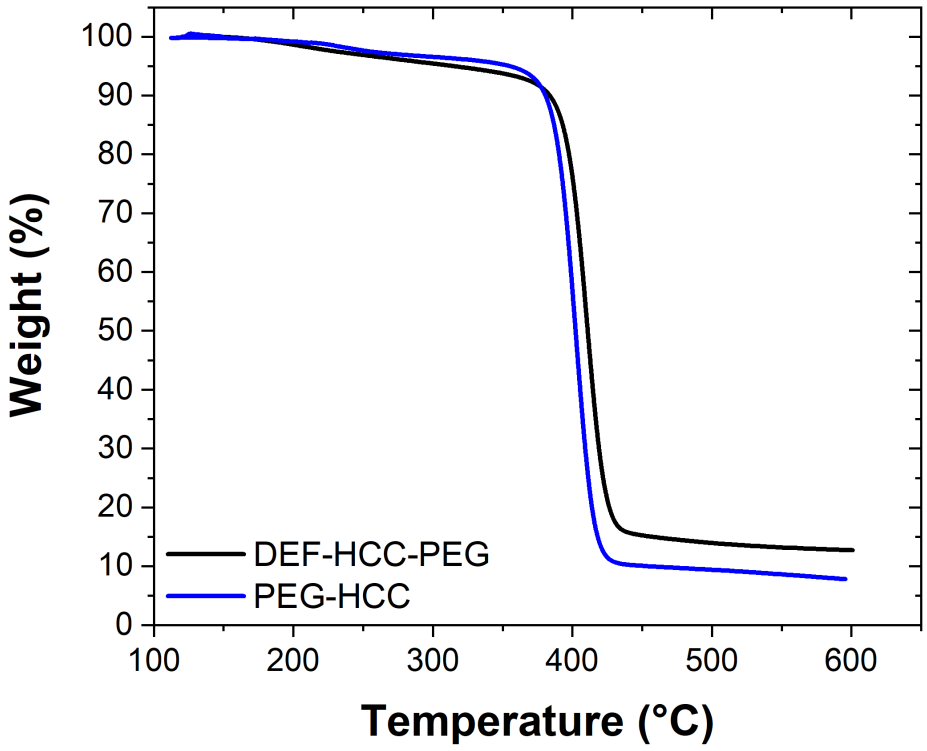


**Figure S8.** Representative TGA of PEG-HCC compared to DEF-HCC-PEG. The thermograms collected indicate the nanomaterials are 81.4% PEG by weight of nanoconjugate and 69.7% PEG/DEF by weight of nanoconjugate (after background subtraction of the HCC weight loss), respectively. Measurements were acquired under $N_{2\,(g)}$ at a ramp rate of 10 °C/min until 800 °C.

## Supporting Methods

### *Characterization of nanoparticle - Calculating DEF and PEG loading of DEF-HCC-PEG*

In order to determine the DEF loading per DEF-HCC-PEG nanoparticle, the nanomaterial was characterized via thermogravimetric analysis (TGA). The acquired data was then compared to the TGA of HCC[1] and PEG-HCCs (Figure S8). TGA is an analytical technique that allows for the weight loss of a material, as a function of temperature, to be determined. Typically, TGA data is collected under $N_{2\,(g)}$ at a ramp rate of 10 °C/min until 800 °C. The oxygen functionalities on the HCC core particle, PEG, and DEF decompose at temperatures < 800 °C; therefore, the weight loss observed by TGA can be used to determine the approximate percent oxygen functionalities, as well as the PEG and DEF loading.

From the weight loss of the HCCs and PEG-HCCs, the molecular weight of the HCC was calculated using similar methodology to that outlined in Samuel, E. *et al*.[2] The number of DEF and PEG moieties covalently bound to the HCCs was quantified by first determining the amount of PEG loaded onto PEG-HCCs. Assuming all of the carboxylic acid sites found on the HCC carbon core are effectively PEGylated, the amount of PEG moieties per PEG-HCC nanoparticle would provide the estimated amount of carboxylic acids per HCC, and, therefore, the number of binding sites for PEG or DEF. It should be noted that this is an approximation since the packing density of PEG vs. PEG/DEF on the HCCs will vary due to the smaller size of DEF (560.7 g/mol) compared to PEG (~5000 g/mol). The estimated moles of PEG per gram of HCC carbon core can be calculated from the thermogram of the PEG-HCC (after background subtraction of the parent particle weight loss):

$$(mass\ PEG\ per\ 1\ g\ carbon\ core\ of\ PEG\text{–}HCC) = \frac{1}{1 - [\frac{\%PEG\ \ of\ PEG\text{–}HCC}{100}]}$$

$$(mol\ PEG\ per\ 1\ g\ carbon\ core\ of\ PEG\text{–}HCC) = \frac{(mass\ PEG\ per\ 1\ g\ carbon\ core\ of\ PEG\text{–}HCC)}{MW\ PEG}$$

Similarly, the approximate mass of PEG and DEF per gram of HCC carbon core was elucidated from the DEF-HCC-PEG thermogram after accounting for the background weight loss of the HCC parent particle:

$$(mass\ PEG\ and\ DEF\ per\ 1\ g\ carbon\ core\ of\ DEF\text{–}HCC\text{–}PEG) = \frac{1}{1 - [\frac{\%PEG\ and\ DEF\ \ of\ DEF\text{–}HCC\text{–}PEG}{100}]}$$

The following system of equations can then be set up to determine the moles of DEF and PEG per gram of DEF-HCC-PEG carbon core, which allows for the number of DEF and PEG moieties per DEF-HCC-PEG nanoparticle to be deduced:

$$\begin{aligned}(mass\ DEF\ and\ PEG\ per\ 1\ g\ carbon\ core\ of\ DEF\text{–}HCC\text{–}PEG) \\ = (mol\ PEG\ of\ DEF\text{–}HCC\text{–}PEG)(MW\ PEG) \\ + (mol\ DEF\ of\ DEF\text{–}HCC\text{–}PEG)(MW\ DEF)\end{aligned}$$

$$(mol\ PEG\ per\ 1\ g\ carbon\ core\ of\ PEG\text{–}HCC)$$
$$= (mol\ PEG\ of\ DEF\text{–}HCC\text{–}PEG) + (mol\ DEF\ of\ DEF\text{–}HCC\text{–}PEG)$$

$$(mass\ DEF\ and\ PEG\ per\ 1\ g\ carbon\ core\ of\ DEF\text{–}HCC\text{–}PEG)$$
$$= (mol\ PEG\ of\ DEF\text{–}HCC\text{–}PEG)(MW\ PEG) + [(mol\ PEG\ of\ PEG\text{–}HCC)$$
$$- (mol\ PEG\ of\ DEF\text{–}HCC\text{–}PEG)](MW\ DEF)$$

$$(mol\ PEG\ of\ DEF\text{–}HCC\text{–}PEG)$$
$$= \frac{(mass\ DEF\ and\ PEG\ per\ 1\ gram\ carbon\ core\ of\ DEF\text{–}HCC\text{–}PEG) - [(mol\ PEG\ of\ PEG\text{–}HCC)(MW\ DEF)]}{[(MW\ PEG) - (MW\ DEF)]}$$

$$(mol\ DEF\ of\ DEF\text{–}HCC\text{–}PEG) = (mol\ PEG\ of\ PEG\text{–}HCC) - (mol\ PEG\ of\ DEF\text{–}HCC\text{–}PEG)$$

$$(PEG\ moieties\ per\ DEF\text{–}HCC\text{–}PEG\ nanparticle)$$
$$= \frac{(mol\ PEG\ per\ 1\ g\ carbon\ core\ of\ DEF\text{–}HCC\text{–}PEG)}{(1\ g/MW\ of\ HCC)}$$

$$(DEF\ moieties\ per\ DEF\text{–}HCC\text{–}PEG\ nanparticle)$$
$$= \frac{(mol\ DEF\ per\ 1\ g\ carbon\ core\ of\ DEF\text{–}HCC\text{–}PEG)}{(1\ g/MW\ of\ HCC)}$$

In a sample of 4 different runs yields average DEF moieties per particle being 58 ± 15 and the average PEG moieties per particle being 75 ± 20.